

# Novel Wearable Seismocardiography and Machine Learning Algorithms Can Assess Clinical Status of Heart Failure Patients

**BACKGROUND:** Remote monitoring of patients with heart failure (HF) using wearable devices can allow patient-specific adjustments to treatments and thereby potentially reduce hospitalizations. We aimed to assess HF state using wearable measurements of electrical and mechanical aspects of cardiac function in the context of exercise.

**METHODS AND RESULTS:** Patients with compensated (outpatient) and decompensated (hospitalized) HF were fitted with a wearable ECG and seismocardiogram sensing patch. Patients stood at rest for an initial recording, performed a 6-minute walk test, and then stood at rest for 5 minutes of recovery. The protocol was performed at the time of outpatient visit or at 2 time points (admission and discharge) during an HF hospitalization. To assess patient state, we devised a method based on comparing the similarity of the structure of seismocardiogram signals after exercise compared with rest using graph mining (graph similarity score). We found that graph similarity score can assess HF patient state and correlates to clinical improvement in 45 patients (13 decompensated, 32 compensated). A significant difference was found between the groups in the graph similarity score metric ( $44.4 \pm 4.9$  [decompensated HF] versus  $35.2 \pm 10.5$  [compensated HF];  $P < 0.001$ ). In the 6 decompensated patients with longitudinal data, we found a significant change in graph similarity score from admission (decompensated) to discharge (compensated;  $44 \pm 4.1$  [admitted] versus  $35 \pm 3.9$  [discharged];  $P < 0.05$ ).

**CONCLUSIONS:** Wearable technologies recording cardiac function and machine learning algorithms can assess compensated and decompensated HF states by analyzing cardiac response to submaximal exercise. These techniques can be tested in the future to track the clinical status of outpatients with HF and their response to pharmacological interventions.

Omer T. Inan, PhD\*  
Maziyar Baran Pouyan,  
PhD\*

Abdul Q. Javaid, PhD  
Sean Dowling, BS  
Mozziyar Etemadi, MD,  
PhD

Alexis Dorier, MS  
J. Alex Heller, MS  
A. Ozan Bicen, PhD  
Shuvo Roy, PhD  
Teresa De Marco, MD  
Livia Klein, MD

\*Drs Inan and Baran Pouyan contributed equally to this work.

**Correspondence to:** Omer T. Inan, PhD, Georgia Institute of Technology, Technology Square Research Bldg, 85 Fifth St, NW, Suite TSB 417, Atlanta, GA 30308. E-mail inan@gatech.edu

**Key Words:** heart failure  
■ hospitalization ■ outpatient  
■ walk test ■ wearable electronic devices

© 2018 American Heart Association, Inc.

### WHAT IS NEW?

- Existing wearable devices are limited to the measurement of actigraphy and ECG signals, which do not provide actionable information for this patient population.
- This article describes an initial study where cardiogenic mechanical signals are measured with a wearable patch, and these signals—measured in the context of exercise—are shown to provide discriminative value in terms of assessing the state of heart failure patients.

### WHAT ARE THE CLINICAL IMPLICATIONS?

- Remote monitoring of patients with heart failure at home using wearable devices can allow titration of care and thereby potentially reduce hospitalizations.
- The approach described here can be leveraged in future studies to monitor patients at home and determine whether the measured signals and their associated features extracted using graph mining algorithms can provide specific and sensitive prediction of worsening state and risk of exacerbation.

**H**ear failure (HF) affects 6.5 million Americans and contributes to ≈300 000 deaths per year.<sup>1</sup> There are >1 million hospital discharges for HF annually and, although many efforts have been made to reduce these hospitalizations, the number has remained relatively constant during the past decade.<sup>1</sup> Moreover, after hospitalization, nearly one fourth of all patients with HF are readmitted within 30 days, and at least half of these readmissions are because of HF.<sup>2</sup> Such hospitalizations greatly impact mortality rates, with the risk of death increasing significantly after hospitalization, and more so with longer duration of hospitalization or repeat hospitalization.<sup>3</sup>

The most common factor associated with HF-related hospitalizations is congestion<sup>4,5</sup> because of elevated left ventricular filling pressures,<sup>6,7</sup> leading to symptoms such as dyspnea, edema, and fatigue that usually occur only a few days before hospitalization.<sup>8</sup> Although treatment during hospitalization reduces signs and symptoms of congestion, even at discharge, nearly half of patients with HF still show such signs and, in fact, this subset of patients has been demonstrated to be at a significantly higher risk of readmission and long-term mortality.<sup>9,10</sup> Accordingly, the monitoring of patients with HF after discharge to proactively manage their care has been recognized as an important need,<sup>11</sup> and multiple tools have been developed and evaluated for this purpose.

Approaches for outpatient HF monitoring have included daily weight measurements and telemonitor-

ing of patient-reported symptoms and vital signs,<sup>12,13</sup> natriuretic peptides,<sup>14</sup> noninvasive bioimpedance monitors,<sup>15</sup> implantable bioimpedance monitors,<sup>16,17</sup> and implantable hemodynamic sensors.<sup>18–20</sup> Other than the direct measurement of intracardiac filling pressures using implantable sensors, none of these approaches has successfully shown improvement in outcomes for patients with HF in large randomized controlled trials. Unfortunately, implantable pressure sensors are invasive, hampering patients' enthusiasm for their use, and the cost of each implant is >\$20 000. Thus, there are millions of patients with HF worldwide who still lack an effective solution for adequate, remote proactive care.

A noninvasive and inexpensive alternative capable of measuring relevant hemodynamic parameters associated with HF worsening could significantly advance home HF management. However, there is no tool available for noninvasive measurement of filling pressures and, thus, a more indirect approach must be designed.

We propose wearable measurements of cardiovascular hemodynamics before and after a controlled dosage of exercise—the 6-minute walk test (6MWT)<sup>21,22</sup>—as a means of noninvasively assessing hemodynamic changes at home.<sup>23</sup> Specifically, we measure the seismocardiogram signal, which represents the vibrations of the chest wall in response to the movement of blood through the arterial tree, and the movement of the heart in the chest.<sup>24,25</sup> The seismocardiogram consists of waves in the time domain that have been shown, using echocardiography as a reference standard, to correspond to aortic valve opening and closing events, as well as the rapid ejection of blood into the aorta.<sup>25</sup> In healthy subjects, exercise leads to substantial changes in the shape and timings of the waveform: for example, the shortening isovolumetric contraction time associated with increased sympathetic tone compresses the seismocardiogram waves in time and thus increases the high frequency components.<sup>26</sup> Our main hypothesis was that the changes in the signal associated with the 6MWT would be significantly less for decompensated patients with HF as compared with compensated patients because the decompensated patients have less cardiovascular reserve to increase their cardiac performance in response to the exercise challenge.

Changes in intracardiac filling pressures relate to changes in stroke volume to maintain the Frank–Starling curve, and therefore assessing changes in cardiac contractility can give an indirect assessment of intracardiac filling pressures.<sup>27</sup> Exertional intolerance is a hallmark of both HF with reduced and preserved ejection fraction and is known to worsen as a patient's condition progresses. One proposed mechanism for the exertional intolerance is the lack of cardiovascular reserve as demonstrated in studies where patients with HF were unable to increase cardiac output with dobutamine infusion.<sup>28</sup> With worsening hemodynamic congestion,

the  $\beta$ -receptors are downregulated, and the sensitivity of the myocardial responsiveness to  $\beta$ -stimulation is blunted; thus, during a stressor (ie, exercise), myocardial contractility cannot be increased successfully to meet the increased body demands.

In this work, we aimed to derive a noninvasive physiological biomarker related to cardiovascular reserve for patients with HF who could be quantified based on wearable seismocardiogram measurements. Specifically, we developed an analytic graph mining-based approach to measure spectral domain similarity of seismocardiogram signals before and after a 6MWT using a wearable patch to provide a noninvasive assessment of the intracardiac hemodynamic changes related to the HF state.

## METHODS

The data that support the findings of this study are available from the corresponding author on reasonable request.

### Wearable Patch Hardware

Unlike impedance based measurements, seismocardiogram is not confounded by fluid shifts in the body and does not require the application of a large number of electrodes on the chest. We measure the seismocardiogram signal using a custom wireless patch<sup>26</sup> mounted at the midsternum that includes an ultralow noise triaxial accelerometer to capture the 3 components of the signal: dorso-ventral, head-to-foot, and lateral accelerations, as shown in Figure 1. The chest vibrations produce a repeatable signal shape that includes peaks corresponding to key events of the cardiac cycle.

The wearable patch (7 cm diameter $\times$ 1 cm thickness, 40 g weight) is mounted to the patient's chest midway between the suprasternal notch and the xiphoid process using 3 Ag/AgCl adhesive-backed gel electrodes (Red Dot 2560, 3M, Maplewood, MN). The patch includes electronics for measuring ECG signals from these electrodes, as well as seismocardiogram signals using a triaxial microelectromechanical systems-based accelerometer (BMA280, Bosch Sensortec GmbH, Reutlingen, Germany). The data from these sensors are sampled at 500 Hz and stored on a micro secure digital card. The overall battery life of the system is 50 hours between charge cycles, thus allowing 24-hour around-the-clock recording including possibly during sleep. The combination of high-resolution acceleration measurements from the chest to facilitate high quality wearable seismocardiogram signal capture and extended battery life to enable long-term monitoring was enabled by cutting edge embedded systems hardware and firmware design. A detailed description of the patch design and validation is provided in Etemadi et al.<sup>26</sup>

### Study Protocol

Under a protocol approved by the University of California, San Francisco, and Georgia Institute of Technology Institutional Review Boards, patients with HF were enrolled from the outpatient HF clinic or from the inpatient cardiology service:

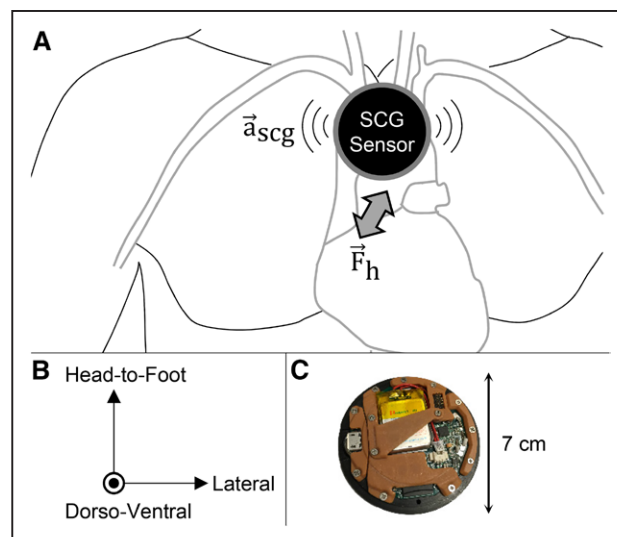


**Figure 1. Seismocardiogram (SCG) and ECG sensing patch.**

**A**, The SCG signal represents the vibrations of the chest wall in response to the movement of the heart and blood with each heartbeat. SCG is measured using a miniature, 3-axis accelerometer, typically positioned on the midsternum. **B**, The SCG signal consists of vibrations in 3 axes: head-to-foot, dorso-ventral, and lateral. **C**, A custom, small, wearable patch for measuring SCG and ECG signals was designed. The patch is placed on the chest using 3 gel adhesive electrodes and stores data locally on a micro secure digital card. The low power design allows for >50 h of continuous recording and use without recharging the battery.

the patients were stage C, not stage D advanced patients with HF. There were no restrictions in terms of ejection fraction, renal function, or use of intravenous medications (including inotropes) for this study. Patients were classified as compensated or decompensated based on the individual clinician assessment, which was derived from patient symptoms and physical examination findings (summarized in the Table). The compensated patients were assessed at the time of the outpatient clinic visit whereas the decompensated patients were assessed on the day of admission during their hospitalization before effective decongestive treatments had been used. Six decompensated patients had the measurements performed both shortly after admission and on the day of discharge.

On providing written informed consent, each subject was fully characterized based on echocardiography, serum biomarkers, symptoms, and medical history. The wearable patch was affixed to each subject's sternum, and after an initial 60 seconds of rest, baseline physiological measurements were obtained. After these measures, the subject performed a 6MWT, where the standard protocol was followed by the study coordinator in terms of describing the procedure to the patient and observing the test.<sup>29</sup> The distance walked by the subject was measured and converted to a percent-predicted 6MWT distance.<sup>29</sup> After completing the 6MWT, the subject was asked to stand still for 5 minutes (recovery phase) while the physiological data were measured using the wearable patch.

**Table. Subject Demographics and Cardiovascular Function Parameters for Study Participants (Grouped by Decompensated and Compensated Patients With Heart Failure)**

	Decompensated (n=13)	Compensated (n=32)	P Value
Sex	11 (85%) M, 2 (15%) F	22 (69%) M, 10 (31%) F	...
Height, cm	176.4±12.1	173.1±7.9	0.28
Weight, kg	93.1±15.3	86.9±21.3	0.35
Age, y	50±16	57±15	0.17
Ejection fraction	20±7	33±14	0.003
NYHA class	1 (8%) III, 12 (92%) IV	4 (12%) I, 12 (38%) II, 9 (28%) III, 7 (22%) IV	...
Dyspnea on exertion (%)	92	50	...
Dyspnea at rest (%)	77	31	...
Orthopnea >2 pillows (%)	92	34	...
Paroxysmal nocturnal dyspnea (%)	69	9	...
Jugular venous pressure, cmH <sub>2</sub> O	14±3	8±2	0.0001
Pulmonary rales (%)	92	19	...
S3 present (%)	46	9	...
Bilateral leg edema (%)	69	25	...
Systolic blood pressure, mmHg	95±15	110±18	0.01
Diastolic blood pressure, mmHg	65±8	75±14	0.02
Heart rate, bpm	95±16	77±16	0.001
Pulmonary edema on chest x-ray (%)	69	N/A	...
BNP, pg/mL	4760±450	380±102	0.0001
Furosemide, mg/d	240±40	80±20	0.0001
Angiotensin-converting enzyme inhibitors/ receptor antagonists (%)	92	100	...
β-Blockers (%)	77	90	...
Mineralocorticoid receptor blockers (%)	77	100	...

Values shown are mean±SD. Statistical significance between groups in values, where applicable, was evaluated using an unpaired *t* test. BNP indicates B-type natriuretic peptide; F, female; M, male; N/A, not applicable; and NYHA, New York Heart Association.

## Noninvasive Physiological Biomarker Quantification

The main goal of proposed methodology is to quantify the spectral domain similarity between the measured seismocardiogram signal (as a surrogate of cardiovascular hemodynamics and cardiac contractility) before and after a 6MWT. We expect that the quantified similarity can allow for phenotyping of patients with HF as compensated or decompensated. Conventional approaches to such a problem typically involve extracting time intervals or amplitude

measurements from the seismocardiogram signals before and after exercise and quantifying the changes in the waveform associated with the 6MWT. However, such approaches can be confounded by noise because they rely on the accurate detection of particular features in the signal, rather than examination of underlying structural characteristics of the signal. The novel methodology we are proposing here involves 2 main steps: (1) pre-processing and feature extraction, and (2) graph similarity computation. By computing the similarity score from the graph representing the structure of the data in the spectral domain, we anticipate that a more robust biomarker can be extracted from the physiological data. The overall workflow for the proposed approach is presented in Figure 2.

## Pre-Processing and Feature Extraction

For pre-processing the signals, first linear filtering was applied on the captured seismocardiogram to reduce out-of-band noise (bandwidth: 0.8–35 Hz [ECG and dorso-ventral seismocardiogram], and 0.8–20 Hz [lateral and head-to-foot seismocardiogram]). These filter bandwidths were selected such that low frequency baseline wander because of respiration and higher frequency noise and artifacts associated with valve closure acoustics were removed from the signals while still preserving the key morphological features of the seismocardiogram. The extracted waveforms from each axis were then averaged to obtain traces with attenuated movement artifacts and uncorrelated noise (Figure 2A). Although such averaging across axes removes the possibility of extracting axis-specific information from the seismocardiogram signal, the focus in this article was to reduce the noise to the extent possible and fuse the 3 axes into the overall graph-based analytics accordingly.

For each subject, the filtered (and averaged) seismocardiogram signals ( $SCG_{3D}$ ) of rest and recovery (for the first 60 seconds) were extracted and separated. Next, we normalized both signals to follow a distribution with zero mean and unity variance. This mitigates any differences in signal amplitude that may result from variability in mechanical coupling of the sensing system to the chest from person to person or moderate compromise in the interface after exercise because of sweating and slight changes in the electrode adhesion. The normalized signals were then segmented using a window size of 1000 ms with 50% overlap, resulting in  $N_{RES}$  and  $N_{REC}$  segmented windows from the rest (*RES*) and recovery (*REC*) phases, respectively. Note that the considered window size was selected heuristically to allow for any cardiovascular signatures to be present within a given window.

Next, we computed the Fourier transform<sup>30</sup> on each window of  $N_{RES}$ . The absolute value of the frequency domain components in different frequency bands were considered as features for each window. For each frequency band, the median of extracted features through all the windows were calculated. This generated a feature vector  $\mathbf{X} = \{x_1, x_2, \dots, x_N\}$  (where *i* indicates *i*th band and *N* denotes the number of frequency bands) representing the spectral characteristics of the entire  $N_{RES}$ . Finally, we applied the same feature extraction approach to calculate the frequency domain features  $\mathbf{Y} = \{y_1, y_2, \dots, y_N\}$  from  $N_{REC}$  (Figure 2B).



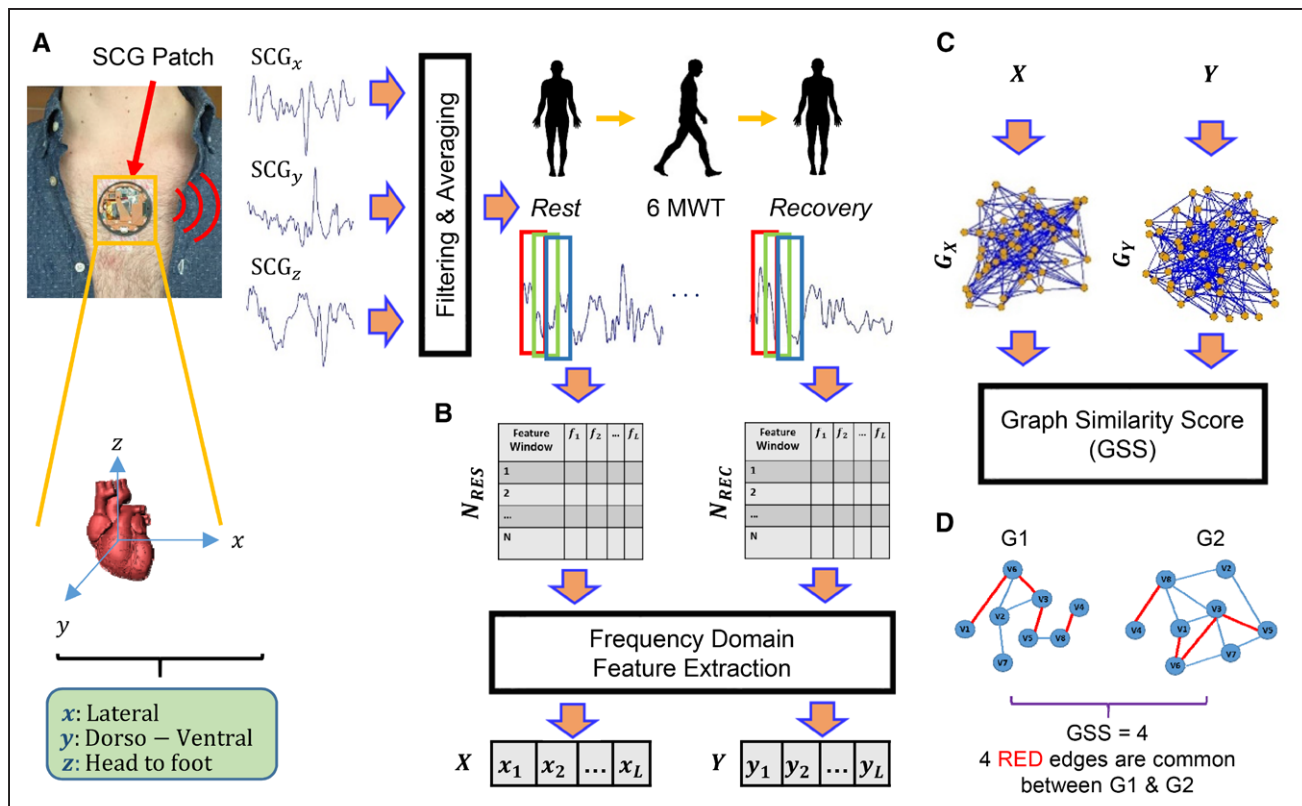


**Figure 2. General overview of the proposed method.**

**A**, The seismocardiogram (SCG) signals (3 axes [dorso-ventral, DV, head-to-foot, HF, and lateral, LAT]) of heart are measured using the custom, wearable patch. Filtering is applied and  $SCG_{3D}$  (a point-by-point average of the 3 axes) is calculated. Then,  $SCG_{3D}$  of rest and recovery segments are windowed and generate  $N_{RES}$  and  $N_{REC}$ . **B**, The  $L$  frequency domain feature sets ( $X$  and  $Y$ ) are computed from  $N_{RES}$  and  $N_{REC}$ . **C**, Two  $k$ -nearest neighbor graphs ( $G_X$  and  $G_Y$ ) are constructed from frequency feature vectors  $X$  and  $Y$ , and GSS is calculated to measure similarity in between rest and recovery states. **D**, An example of graph similarity score (GSS) calculation between 2 illustrative graphs. 6MWT indicates 6-minute walk test.

## Graph Similarity Score Computation

To quantify structural changes in the seismocardiogram signal before and after a 6MWT (rest and recovery phases), we computed the similarity between the extracted feature vectors  $X$  and  $Y$ . Although there are several traditional techniques such as Minkowski and correlation-based similarity scores<sup>31</sup> to measure similarity, all of them have 2 major drawbacks: (1) their practical efficiency reduces by increasing vector dimensionality because of the curse of dimensionality<sup>32</sup> (ie, a phenomenon in high dimensional space which prevents common data organization to be effective); and (2) they do not consider pertinent dependencies among measured features. Therefore, to overcome these challenges, we used an approach that is commonly used in graph theory. We modeled each feature vector using a  $k$ -nearest neighbor graph<sup>33</sup> and then calculated structural similarity between these graphs using a simple graph-matching approach. This method overcomes the related drawbacks to the traditional techniques because it models possible dependencies among frequency features using a network structure. We used a value of  $k=20$ , but also computed the results with  $k=10$  and 30 without any substantial differences in the final results.

We used both feature vectors  $X$  and  $Y$  to construct 2  $k$ -nearest neighbor graph graphs per subject ( $G_X$  and  $G_Y$ ).

An important benefit of the graph mining is that the feature vectors can be readily visualized in lower dimensional (ie, 2-dimensional) space while preserving the underlying geometric relationships between the features. We represent the features of  $X$  as vertices in the graph and connect each vertex to its  $k$  nearest neighboring vertices using Euclidean distance. This process makes an unweighted-undirected graph  $G_X$  from  $X$ . The same process is performed to extract  $G_Y$  from  $Y$  (Figure 2C).

Finally, we count the number of common edges that exist in both graphs and consider that as a structural similarity between 2 graphs. In this article, we refer to this as the graph similarity score (GSS). Unlike traditional techniques, GSS is able to capture the structural similarity of the seismocardiogram signal between rest and recovery phases because it considers possible dependencies of features using applied graph mining. Figure 2D shows a simple example of GSS calculation using 2 illustrative graphs. In this example, the GSS between the 2 graphs is 4 because 4 common edges exist between them.

## Statistical Analysis

The calculated GSS between rest and recovery phases for the decompensated versus compensated patients were compared

using the Mann–Whitney  $U$  test. In addition, the Wilcoxon signed-rank test was used to compare the changes in GSS for the patients with HF from admit to discharge (longitudinal study). The demographics of patients in the decompensated and compensated groups were compared using Student  $t$  test. The 6MWT walking distances, percent-predicted walking distances, and heart rates for the patients with HF from admit to discharge (longitudinal study) were compared using a paired  $t$  test. Means are expressed as mean $\pm$ SD.

## RESULTS

Of the 45 subjects enrolled in the study, 13 were decompensated hospitalized (ejection fraction:  $0.24\pm0.11$ ) and 32 were compensated ambulatory (ejection fraction:  $0.35\pm0.15$ ) patients with HF. There were no significant baseline differences between the groups in terms of demographics (ie, age, height, and weight;  $P>0.05$  based on Student  $t$  test).

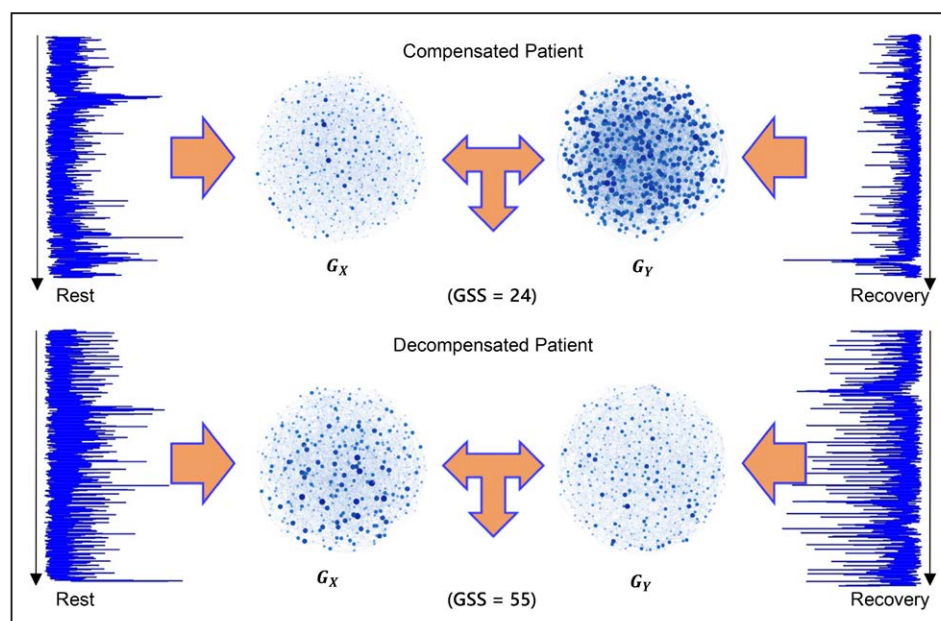
### GSS Is Significantly Higher in Decompensated Than in Compensated Patients With HF, Suggesting a Reduced Cardiovascular Reserve for Decompensated Patients

Figure 3 shows representative seismocardiogram ensemble averages from rest and immediately after the 6MWT (recovery phase) and related  $G_x$  and  $G_y$  graphs

of a decompensated patient with HF (bottom) and a compensated patient (top). For the decompensated patient, the GSS value between  $G_x$  and  $G_y$  is 55 and for the compensated patient, the calculated GSS value is 24. This result indicates the higher similarity in contractility and cardiovascular hemodynamics between rest and recovery phases for decompensated patients in comparison with compensated patients.

These single subject representative results are consistent with the overall findings from all participants, summarized in Figure 4 (compensated versus decompensated). The calculated GSS values were significantly higher for the decompensated compared with compensated patients:  $44.4\pm4.9$  versus  $35.2\pm10.6$ , respectively,  $P<0.01$ .

To understand the effects of the time duration during recovery (nominally selected as 60 seconds in this article) that is selected at the recovery phase to then compare against the rest phase, we recalculated the GSS metric with varying durations of the recovery phase for all the subjects and computed corresponding  $P$  values. The best result (most significant value) was found when the initial 1 minute of recovery was compared with rest phase. Incorporating a longer time interval (eg, 5 minutes) after the 6MWT reduces the differences between the decompensated and compensated groups because the cardiovascular system recovers back to the resting state for both groups of patients after exercise after a few minutes.



**Figure 3. Calculated graph similarity score (GSS) for representative decompensated and compensated patients.**

Representative seismocardiogram (SCG) time traces from rest and recovery after the 6-minute walk test (6MWT) and associated  $G_x$  and  $G_y$  graphs of a compensated patient with heart failure (**top**) and a decompensated patient (**bottom**). For the decompensated patient, the GSS value is 55 and for the compensated patient, the corresponding value is 24. This result demonstrates the higher similarity in SCG waveform structure between rest and recovery phases of the decompensated patient in comparison with compensated patient. The graphs also demonstrate the higher similarity for decompensated versus compensated states visually.

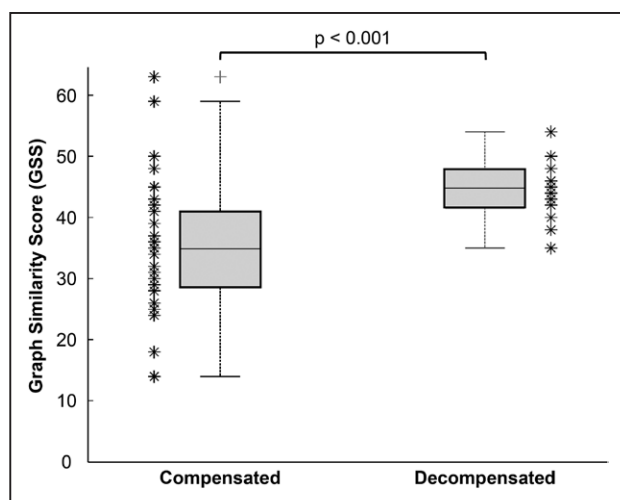


**Figure 4. Overall statistical analysis of the graph similarity score (GSS) metric from all patients grouped by clinical state (compensated vs decompensated).**

The GSS between rest and recovery phases was significantly higher for the decompensated patients as compared with compensated;  $n=45$  subjects ( $P<0.001$ ).

The absolute and percent-predicted 6MWT distance were significantly higher for the compensated compared with decompensated patients:  $369\pm102$  m versus  $250\pm130$  m for the compensated and decompensated patients, respectively,  $P<0.01$ ; and  $71\pm25\%$  versus  $41\pm20\%$ , for the compensated and decompensated, respectively,  $P<0.01$ .

We computed GSS across NYHA class for all subjects, and we found a monotonic increase with respect to class. Patients with NYHA class I to IV symptoms had the following GSS values:  $24.3\pm4.3$ ,  $36.8\pm11.4$ ,  $37\pm10$ ,

and  $42.5\pm6.0$ . Statistical significance was only found in the differences between class I and all other classes.

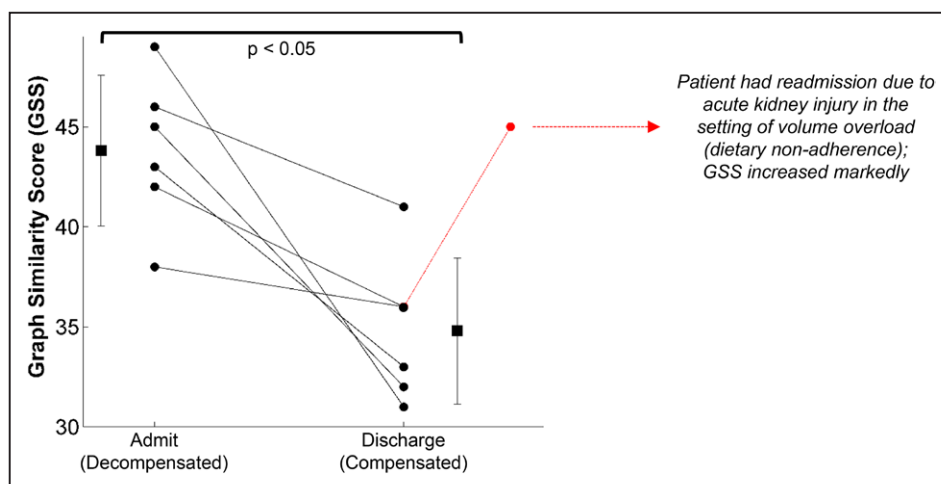
### GSS in Treated Decompensated Patients With HF Decreases From Admission to Discharge, Indicating Improvement in Cardiovascular Reserve

Figure 5 depicts results from the subset of decompensated patients with HF who participated in 2 sessions (longitudinal cases). The GSS between the rest and recovery phases was significantly higher on admission compared with discharge:  $44\pm4.1$  (admitted) versus  $35\pm3.9$  (discharged);  $P<0.05$ . In addition, 1 patient had a third visit as well. As presented in Figure 5, that patient had an increased GSS in the third visit because of readmission due to acute kidney injury and associated volume overload.

For these same patients, the absolute and percent-predicted 6MWT distance also increased from  $90.9\pm48.1$  m to  $115.5\pm37.3$  m ( $P=0.33$ ) and  $30\pm19\%$  to  $36\pm16\%$  ( $P=0.08$ ), respectively, but the increases were not significant. The changes in heart rate in response to the 6MWT exercise increased slightly from admit to discharge ( $12.2\pm10.6$  bpm to  $13.5\pm11.6$  bpm;  $P=0.66$ ), but these increases were also not significant.

## DISCUSSION

We have presented data demonstrating that a small, lightweight wearable patch for measuring changes in GSS in response to a controlled exercise protocol can



**Figure 5. Graph similarity score (GSS) for heart failure inpatients decreases from admit to discharge.**

Longitudinal results from a subset of the inpatient population for which the 6-minute walk test data were obtained when the subjects were admitted (left) and on discharge (right) after treatment. For all patients, GSS decreased at discharge as compared with when first admitted. Thus, as the decompensated patients were treated, longitudinal changes in the physiological response to exercise were observed in a consistent manner with the cross-sectional data from the overall cohort of subjects. One patient had a third visit as well and showed markedly increased GSS because of readmission due to acute kidney injury and volume overload.

differentiate between decompensated and compensated patients with HF. The results are consistent with physiological expectations: the decompensated (and more congested) patients have less cardiovascular reserve, and thus are not able to modulate their hemodynamics or cardiac contractility as effectively as the compensated patients during exercise. Importantly, for the 1 patient who was readmitted with abnormal volume status, a higher value of GSS (indicating reduced cardiovascular reserve) was found. For the longitudinal study evaluating within-subject improvements from admission to discharge, the calculated GSS showed a significant improvement (decreasing in GSS value) with treatment while other factors such as heart rate response to exercise, 6MWT distance, and percent-predicted distance did not show significant improvement. This result suggests that the GSS metric may be more sensitive to changes in patient status than these other more traditional measures of the responses of the cardiovascular system to exercise. Because the 6MWT distance itself has already been validated as a prognostic for patients with HF, these results are promising and motivate further studies for evaluating the technology in larger populations of patients with HF.

Although  $\beta$ -blockers impact cardiac contractility and thus might affect the seismocardiogram data, the differences in total  $\beta$ -blocker use were not significant between the 2 groups studied (decompensated and compensated patients). A total of 77% of the decompensated and 90% of the compensated patients were using  $\beta$ -blockers. Thus, we do not expect that the GSS differences between the 2 groups were confounded by  $\beta$ -blocker use. Future studies should analyze the effects of  $\beta$ -blocker dosage on seismocardiogram data and GSS.

Because the proposed graph analytic technique works based on multiple extracted features from the seismocardiogram signal, it is more robust to motion artifacts, day-to-day variability, and noise compared with conventional peak detection approaches. This machine learning algorithm can also potentially be implemented in a real-time monitoring system to evaluate the status of patients with HF because its time complexity is low. Indeed, the concept of using graph analytics as compared with single features of physiological signals can be applied more broadly to other cardiovascular signals as well, such as impedance cardiogram or photoplethysmogram waveforms. Conventional feature extraction approaches rely on the accurate detection of peaks in the time or frequency domain, and these peaks can often be corrupted by motion artifacts and other disturbances in practical recordings outside of laboratory or clinical settings. Tracking changes in the signals in the feature space, as enabled by GSS for example, reduces the burden on the extraction methods for each individual feature because the overall cloud of features is

tracked in high-dimensional space rather than a single feature alone.

The research has several limitations that should be noted. Currently, the differentiation between the groups (compensated and decompensated) was not sufficiently large to facilitate classification of patient state; future work will be needed to enhance the ability of the algorithms to perform such classification. The approach requires the patient to perform a 6MWT and to stand still for at least 60 seconds before and after the test, which may be inconvenient. Nevertheless, such a procedure may only be required once per day or every other day, and it is possible that in future studies a less obtrusive stressor may be used while still preserving the accuracy of the derived features. In future work, we will investigate such approaches and define a dose response curve for decompensated and compensated patients relating GSS changes to activity dosage (eg, in units of estimated energy expenditure, distance walked, or time walked). Another limitation is the relatively small population of patients in the longitudinal study. Although significant results were obtained, the number of participants is small and must be expanded in future studies to better evaluate the potential advantage of this approach compared with heart rate and activity monitors. Specifically, this small single-center study will require replication in larger prospective trials in multiple sites. An important characteristic of the patch system described here is that, in addition to hemodynamic measurements, high-quality ECG-based heart rate and rhythm and accelerometer-based activity data are also inherently collected. Thus, the seismocardiogram-derived features are supplementing existing technologies rather than attempting to replace them, providing the opportunity for fused metrics of improving or worsening condition using a single wearable device. In addition, the compensated/decompensated status of each patient was known to the investigators because this was a first proof-of-concept study; future studies should use a blinded assessment to determine whether GSS can predict clinical status. Finally, the measurements described in this article were obtained in a controlled, clinical environment only, and the results at home in unsupervised settings may be of lower quality than the data obtained here. In future work, the wearable patch will be tested in patients at home to determine whether markers of increasing congestion can be successfully derived toward ultimately titrating care based on the noninvasive physiological measurements from the system.

## CONCLUSIONS

We have shown that a wearable device capable of recording electrical and mechanical aspects of cardiac function and graph mining techniques analyzing cardiac response to submaximal exercise can be used to



identify compensated and decompensated HF states and to track the clinical course of the patients. These techniques can be tested in the future to track the clinical status of outpatients with HF and their response to pharmacological interventions.

## SOURCES OF FUNDING

Research reported in this publication was supported, in part, by the National Institute on Aging under Award Number R56AG048458 and the National Heart, Lung and Blood Institute under R01HL130619. The content is solely the responsibility of the authors and does not necessarily represent the official views of the National Institutes of Health.

## DISCLOSURES

Dr Inan has consulting/advisory board relationships with PhysioWave, Inc. The other authors report no conflicts.

## AFFILIATIONS

From the School of Electrical and Computer Engineering, Georgia Institute of Technology, Atlanta (O.T.I., M.B.P., A.Q.J., A.D., A.O.B.); Division of Cardiology (S.D., T.D.M., L.K.) and Department of Bioengineering and Therapeutic Sciences (S.R.), University of California, San Francisco; and Department of Anesthesiology and Department of Biomedical Engineering, Northwestern University, Chicago, IL (M.E., J.A.H.).

## FOOTNOTES

Received June 13, 2017; accepted December 15, 2017.

Guest Editor for this article was W. H. Wilson Tang, MD.

*Circ Heart Fail* is available at <http://circheartfailure.ahajournals.org>.

## REFERENCES

- Benjamin EJ, Blaha MJ, Chiuve SE, Cushman M, Das SR, Deo R, de Ferranti SD, Floyd J, Fornage M, Gillespie C, Isasi CR, Jiménez MC, Jordan LC, Judd SE, Lackland D, Lichtman JH, Lisabeth L, Liu S, Longenecker CT, Mackey RH, Matsushita K, Mozaffarian D, Mussolino ME, Nasir K, Neumar RW, Palaniappan L, Pandey DK, Thiagarajan RR, Reeves MJ, Ritchey M, Rodriguez CJ, Roth GA, Rosamond WD, Sasson C, Towfighi A, Tsao CW, Turner MB, Virani SS, Voeks JH, Willey JZ, Wilkins JT, Wu JH, Alger HM, Wong SS, Muntner P; American Heart Association Statistics Committee and Stroke Statistics Subcommittee. Heart Disease and Stroke Statistics-2017 Update: a report from the American Heart Association. *Circulation*. 2017;135:e146–e603. doi: 10.1161/CIR.0000000000000485.
- Dharmarajan K, Hsieh AF, Lin Z, Bueno H, Ross JS, Horwitz LJ, Barreto-Filho JA, Kim N, Bernheim SM, Suter LG, Drye EE, Krumholz HM. Diagnoses and timing of 30-day readmissions after hospitalization for heart failure, acute myocardial infarction, or pneumonia. *JAMA*. 2013;309:355–363. doi: 10.1001/jama.2012.216476.
- Solomon SD, Dobson J, Pocock S, Skali H, McMurray JJ, Granger CB, Yusuf S, Swedberg K, Young JB, Michelson EL, Pfeffer MA; Candesartan in Heart failure: Assessment of Reduction in Mortality and morbidity (CHARM) Investigators. Influence of nonfatal hospitalization for heart failure on subsequent mortality in patients with chronic heart failure. *Circulation*. 2007;116:1482–1487. doi: 10.1161/CIRCULATIONAHA.107.696906.
- Fonarow GC; ADHERE Scientific Advisory Committee. The Acute De-compensated Heart Failure National Registry (ADHERE): opportunities to improve care of patients hospitalized with acute decompensated heart failure. *Rev Cardiovasc Med*. 2003;4(suppl 7):S21–S30.
- Cleland JG, Swedberg K, Follath F, Komajda M, Cohen-Solal A, Aguilar JC, Dietz R, Gavazzi A, Hobbs R, Korewicki J, Madeira HC, Moiseyev VS, Preda I, van Gilst WH, Widimsky J, Freemantle N, Eastaugh J, Mason J; Study Group on Diagnosis of the Working Group on Heart Failure of the European Society of Cardiology. The EuroHeart Failure survey programme—a survey on the quality of care among patients with heart failure in Europe. Part 1: patient characteristics and diagnosis. *Eur Heart J*. 2003;24:442–463.
- Adamson PB, Magalski A, Braunschweig F, Böhm M, Reynolds D, Steinhilber D, Luby A, Linde C, Ryden L, Cremers B, Takle T, Bennett T. Ongoing right ventricular hemodynamics in heart failure: clinical value of measurements derived from an implantable monitoring system. *J Am Coll Cardiol*. 2003;41:565–571.
- Zile MR, Bennett TD, St John Sutton M, Cho YK, Adamson PB, Aaron MF, Aranda JM Jr, Abraham WT, Smart FW, Stevenson LW, Kueffer FJ, Bourge RC. Transition from chronic compensated to acute decompensated heart failure: pathophysiological insights obtained from continuous monitoring of intracardiac pressures. *Circulation*. 2008;118:1433–1441. doi: 10.1161/CIRCULATIONAHA.108.783910.
- Gattis WA, O'Connor CM, Gallup DS, Hasselblad V, Gheorghiade M; IMPACT-HF Investigators and Coordinators. PredischARGE initiation of carvedilol in patients hospitalized for decompensated heart failure: results of the Initiation Management PredischARGE: Process for Assessment of Carvedilol Therapy in Heart Failure (IMPACT-HF) trial. *J Am Coll Cardiol*. 2004;43:1534–1541. doi: 10.1016/j.jacc.2003.12.040.
- Ambrosy AP, Pang PS, Khan S, Konstam MA, Fonarow GC, Traver B, Maggioni AP, Cook T, Swedberg K, Burnett JC Jr, Grinfeld L, Udelson JE, Zannad F, Gheorghiade M; EVEREST Trial Investigators. Clinical course and predictive value of congestion during hospitalization in patients admitted for worsening signs and symptoms of heart failure with reduced ejection fraction: findings from the EVEREST trial. *Eur Heart J*. 2013;34:835–843. doi: 10.1093/eurheartj/ehs444.
- Zile MR, Bennett TD, El Hajj S, Kueffer FJ, Baicu CF, Abraham WT, Bourge RC, Stevenson LW. Intracardiac pressures measured using an implantable hemodynamic monitor: relationship to mortality in patients with chronic heart failure. *Circ Heart Fail*. 2017;10:3594–3602.
- Bui AL, Fonarow GC. Home monitoring for heart failure management. *J Am Coll Cardiol*. 2012;59:97–104. doi: 10.1016/j.jacc.2011.09.044.
- Chaudhry SI, Wang Y, Concato J, Gill TM, Krumholz HM. Patterns of weight change preceding hospitalization for heart failure. *Circulation*. 2007;116:1549–1554. doi: 10.1161/CIRCULATIONAHA.107.690768.
- Ong MK, Romano PS, Edgington S, Aronow HU, Auerbach AD, Black JT, De Marco T, Escarce JJ, Evangelista LS, Hanna B, Ganiats TG, Greenberg BH, Greenfield S, Kaplan SH, Kimchi A, Liu H, Lombardo D, Mangione CM, Sadeghi B, Sadeghi B, Sarrafzadeh M, Tong K, Fonarow GC; Better Effectiveness After Transition—Heart Failure (BEAT-HF) Research Group. Effectiveness of remote patient monitoring after discharge of hospitalized patients with heart failure: the Better Effectiveness After Transition – Heart Failure (BEAT-HF) Randomized Clinical Trial. *JAMA Intern Med*. 2016;176:310–318. doi: 10.1001/jamainternmed.2015.7712.
- Felker GM, Ahmad T, Anstrom KJ, Adams KF, Cooper LS, Ezekowitz JA, Fiuzat M, Houston-Miller N, Januzzi JL, Leifer ES, Mark DB, Desvigne-Nickens P, Paynter G, Piña IL, Whellan DJ, O'Connor CM. Rationale and design of the GUIDE-IT study: guiding evidence based therapy using biomarker intensified treatment in heart failure. *JACC Heart Fail*. 2014;2:457–465. doi: 10.1016/j.jchf.2014.05.007.
- Packer M, Abraham WT, Mehra MR, Yancy CW, Lawless CE, Mitchell JE, Smart FW, Bijou R, O'Connor CM, Massie BM, Pina IL, Greenberg BH, Young JB, Fishbein DP, Hauptman PJ, Bourge RC, Strobeck JE, Murali S, Schocken D, Teerlink JR, Levy WC, Trupp RJ, Silver MA; Prospective Evaluation and Identification of Cardiac Decompensation by ICG Test (PREDICT) Study Investigators and Coordinators. Utility of impedance cardiography for the identification of short-term risk of clinical decompensation in stable patients with chronic heart failure. *J Am Coll Cardiol*. 2006;47:2245–2252. doi: 10.1016/j.jacc.2005.12.071.
- Yu CM, Wang L, Chau E, Chan RH, Kong SL, Tang MO, Christensen J, Stadler RW, Lau CP. Intrathoracic impedance monitoring in patients with heart failure: correlation with fluid status and feasibility of early warning preceding hospitalization. *Circulation*. 2005;112:841–848. doi: 10.1161/CIRCULATIONAHA.104.492207.
- Abraham WT, Compton S, Haas G, Foreman B, Canby RC, Fishel R, McRae S, Toledo GB, Sarkar S, Hettrick DA; FAST Study Investigators. Intrathoracic

- impedance vs daily weight monitoring for predicting worsening heart failure events: results of the Fluid Accumulation Status Trial (FAST). *Congest Heart Fail*. 2011;17:51–55. doi: 10.1111/j.1751-7133.2011.00220.x.
18. Bourge RC, Abraham WT, Adamson PB, Aaron MF, Aranda JM Jr, Magalski A, Zile MR, Smith AL, Smart FW, O'Shaughnessy MA, Jessup ML, Sparks B, Naftel DL, Stevenson LW; COMPASS-HF Study Group. Randomized controlled trial of an implantable continuous hemodynamic monitor in patients with advanced heart failure: the COMPASS-HF study. *J Am Coll Cardiol*. 2008;51:1073–1079. doi: 10.1016/j.jacc.2007.10.061.
  19. Ritzema J, Melton IC, Richards AM, Crozier IG, Frampton C, Doughty RN, Whiting J, Kar S, Eigler N, Krum H, Abraham WT, Troughton RW. Direct left atrial pressure monitoring in ambulatory heart failure patients: initial experience with a new permanent implantable device. *Circulation*. 2007;116:2952–2959. doi: 10.1161/CIRCULATIONAHA.107.702191.
  20. Abraham WT, Stevenson LW, Bourge RC, Lindenfeld JA, Bauman JG, Adamson PB; CHAMPION Trial Study Group. Sustained efficacy of pulmonary artery pressure to guide adjustment of chronic heart failure therapy: complete follow-up results from the CHAMPION randomised trial. *Lancet*. 2016;387:453–461. doi: 10.1016/S0140-6736(15)00723-0.
  21. Cahalin LP, Mathier MA, Semigran MJ, Dec GW, DiSalvo TG. The six-minute walk test predicts peak oxygen uptake and survival in patients with advanced heart failure. *Chest*. 1996;110:325–332.
  22. Brooks GC, Vittinghoff E, Iyer S, Tandon D, Kuhar P, Madsen KA, Marcus GM, Pletcher MJ, Olgin JE. Accuracy and usability of a self-administered 6-minute walk test smartphone application. *Circ Heart Fail*. 2015;8:905–913. doi: 10.1161/CIRCHEARTFAILURE.115.002062.
  23. Klein L. Treating hemodynamic congestion is the key to prevent heart failure hospitalizations. *JACC Heart Fail*. 2016;4:345–347. doi: 10.1016/j.jchf.2016.03.004.
  24. Zanetti JM, Salerno DM. Seismocardiography: a technique for recording precordial acceleration. *Computer-Based Medical Systems*, 1991 *Proceedings of the Fourth Annual IEEE Symposium*. Baltimore, MD. 1991:4–9.
  25. Inan OT, Migeotte PF, Park KS, Etemadi M, Tavakolian K, Casanella R, Zanetti J, Tank J, Funtova I, Prisk GK, Di Rienzo M. Ballistocardiography and seismocardiography: a review of recent advances. *IEEE J Biomed Health Inform*. 2015;19:1414–1427. doi: 10.1109/JBHI.2014.2361732.
  26. Etemadi M, Inan OT, Heller JA, Hersek S, Klein L, Roy S. A wearable patch to enable long-term monitoring of environmental, activity and hemodynamics variables. *IEEE Trans Biomed Circuits Syst*. 2016;10:280–288. doi: 10.1109/TBCAS.2015.2405480.
  27. Steimle AE, Stevenson LW, Chelimsky-Fallick C, Fonarow GC, Hamilton MA, Moriguchi JD, Kartashov A, Tillisch JH. Sustained hemodynamic efficacy of therapy tailored to reduce filling pressures in survivors with advanced heart failure. *Circulation*. 1997;96:1165–1172.
  28. Norman HS, Oujiri J, Larue SJ, Chapman CB, Margulies KB, Sweitzer NK. Decreased cardiac functional reserve in heart failure with preserved systolic function. *J Card Fail*. 2011;17:301–308. doi: 10.1016/j.cardfail.2010.11.004.
  29. ATS Committee on Proficiency Standards for Clinical Pulmonary Function Laboratories. ATS statement: guidelines for the six-minute walk test. *Am J Resp Crit Care Med*. 2002;166:111–117.
  30. Brigham EO. *The Fast Fourier Transform and Its Applications*. Englewood Cliffs, NJ: Prentice Hall; 1988.
  31. Jain AK, Murty MN, Flynn PJ. Data clustering: a review. *ACM Computing Surveys (CSUR)*. 1999;31:264–323.
  32. Bishop CM. *Pattern Recognition and Machine Learning (Information Science and Statistics)*. New York, NY: Springer-Verlag; 2006.
  33. Dong W, Moses C, Li K. Efficient k-nearest neighbor graph construction for generic similarity measures. *Proceedings of the 20th International Conference on World Wide Web (WWW '11)*, Hyderabad, India 2011; 577–586.

### Novel Wearable Seismocardiography and Machine Learning Algorithms Can Assess Clinical Status of Heart Failure Patients

Omer T. Inan, Mazyar Baran Pouyan, Abdul Q. Javaid, Sean Dowling, Mozziyar Etemadi, Alexis Dorier, J. Alex Heller, A. Ozan Bicen, Shuvo Roy, Teresa De Marco and Liviu Klein

*Circ Heart Fail.* 2018;11:

doi: 10.1161/CIRCHEARTFAILURE.117.004313

*Circulation: Heart Failure* is published by the American Heart Association, 7272 Greenville Avenue, Dallas, TX 75231

Copyright © 2018 American Heart Association, Inc. All rights reserved.

Print ISSN: 1941-3289. Online ISSN: 1941-3297

The online version of this article, along with updated information and services, is located on the World Wide Web at:

<http://circheartfailure.ahajournals.org/content/11/1/e004313>

**Permissions:** Requests for permissions to reproduce figures, tables, or portions of articles originally published in *Circulation: Heart Failure* can be obtained via RightsLink, a service of the Copyright Clearance Center, not the Editorial Office. Once the online version of the published article for which permission is being requested is located, click Request Permissions in the middle column of the Web page under Services. Further information about this process is available in the [Permissions and Rights Question and Answer](#) document.

**Reprints:** Information about reprints can be found online at:  
<http://www.lww.com/reprints>

**Subscriptions:** Information about subscribing to *Circulation: Heart Failure* is online at:  
<http://circheartfailure.ahajournals.org/subscriptions/>